International Journal of Thermophysics, Vol. 14, No. 2, 1993

P–V–T–x Measurements of Aqueous Mixtures at Supercritical Conditions

I. M. Abdulagatov,[1] A. R. Bazaev,[1] and A. E. Ramazanova[1]

Received December 8, 1992

We report *P–V–T–x* measurements for five binary systems: water + methane, water + *n*-hexane, water + *n*-octane, water + benzene, and water + nitrogen at supercritical conditions for several compositions. The experimental data were obtained along isotherms with a phase-equilibrium cell designed for accurate measurements at pressures up to 100 MPa. The uncertainties in temperature, pressure, density, and concentration are ±0.01 K, ±0.2%, ±0.2%, and ±0.002 mole fractions, respectively. The behavior of the second virial coefficient, the excess volume, and the excess Gibbs free energy is also discussed.

KEY WORDS: aqueous mixtures; compressibility factor; equation of state; excess Gibbs free energy; excess volume; hydrocarbons; supercritical fluids.

1. INTRODUCTION

In many chemical processes and especially in petroleum engineering, where mixtures of water with hydrocarbons are encountered, phase behavior may be of great practical significance. Fluid mixtures at elevated temperatures and pressures are of interest for technology, geochemistry, and studies of molecular interactions. Examples of recent technical applications are supercritical extraction [1, 2], supercritical separation processes [3], supercritical oxidation [4], and problems in geochemistry [5]. The production of energy alternatives, such as synthetic gas and fuel, and hydrolysis of heavy oils and tar require a knowledge of the properties of aqueous mixtures at high temperatures and high pressures. The need for thermophysical-property data for aqueous solutions at high temperatures and pressures in different areas of science and engineering has recently been discussed in more detail by Levelt Sengers [6].

[1] Institute for Geothermal Problems, Dagestan Branch of the Russian Academy of Sciences, Kalinina 39-A, 367024 Makhachkala, Russia.

0195-928X/93/0300-0231$07.00/0 © 1993 Plenum Publishing Corporation

Aside from possible industrial applications, mixtures of water and hydrocarbons are interesting from the point of view of interactions between two molecules representative of polar and nonpolar liquids. A study of the thermodynamic properties of mixtures of water and alkanes offers the possibility of investigating the effect of a gradual increase in chain length of *n*-alkanes on the critical locus and on phase equilibria. Previous studies offer the possibility of concluding how the shape of the critical locus of mixtures of water and *n*-alkanes changes with the carbon number of the alkanes [7–9].

Many questions of the modern theory of critical phenomena are related to the behavior of P–V–T–x properties of fluid mixtures near vapor–liquid critical lines [10, 11]. For example, the derivatives dT_c/dx, dP_c/dx, and $d\rho_c/dx$, where T_c is the critical temperature, P_c the critical pressure, ρ_c the critical pressure, ρ_c the critical density, and x the concentration, determine the qualitative behavior of thermodynamic properties such as the isothermal compressibility $K_{T,X}$ and the isochoric specific heat $C_{V,X}$ near the critical locus [1, 6, 12].

The purpose of the present paper is to report $P-V-T-x$ measurements for mixtures of water with hydrocarbons and with nitrogen. The phase boundaries of several mixtures of water with hydrocarbons at high temperatures and pressures have been determined by Bröllos et al. [13], Yiling et al. [14], Japas and Franck [15], and Rebert and Kay [16]. Gas–gas equilibria of the second type have been determined in water + methade [17, 18], water + ethane [19], water + propane [20, 21], water + *n*-butane [14, 19], water + *n*-pentane [22], water + *n*-hexane [14], water + *n*-heptane [13, 22, 23], and water + benzene [24]. However, P–V–T–x data in the vapor-phase region for water + methane, water + *n*-hexane, water + *n*-octane, water + benzene, and water + nitrogen are not available.

Phase equilibria in water + *n*-hexane have been investigated only at high concentrations [7] and at moderate pressures [25]. For water + nitrogen high-pressure phase equilibria and P–V–T–x data have been determined in the homogeneous supercritical region at 673 K [15]. Critical curves and two-phase equilibrium surfaces in P–T–X space have been determined for water + methane [28] and water + *n*-butane [29].

2. EXPERIMENTS

The experiments were performed with a constant-volume piezometer in a precision thermostat. The measurements were made at temperatures up to 663 K. The volume of the piezometer was determined experimentally from the weight of the amount of water in the piezometer at a constant

temperature and the measured volume of the connecting fittings. The volume of the piezometer was determined with an uncertainty of $\pm 0.1\,\%$.

The experimental apparatus and procedures have been described in detail in previous publications [30, 31], and only a brief description here suffices. The apparatus consists of four parts, namely, a piezometer, an air thermostat, a system for filling samples, and a system for taking samples for analysis. The piezometer was made from a heat- and corrosive-resistant high-strength alloy (EI-437B4) and has a cylindrical form. It has an internal diameter of 30 mm and an outside diameter of 70 mm. The working volume of the piezometer is 33 cm^3. On one of the ends of the piezometer a diaphragm-type null indicator is mounted, and on the other end, a valve. To reach equilibriuim fast, the sample was stirred with a steel ball bearing which was rotated rapidly in the sample. The known linear expansion coefficient of the alloy was used to correct the volume of the piezometer as a function of temperature and pressure.

The piezometer is located horizontally in the center of an air thermostat. The air thermostat has double walls and it has an inside volume of 65 cm^3. The electrical heater for setting the desired temperature inside the thermostat is located between the walls of the thermostat. The regulating heater was mounted inside the thermostat to avoid thermal losses. The thermostat temperature is controlled automatically to within ± 1 mK. The temperature is measured with a 10-Ω Pt thermometer mounted in the vicinity of the piezometer. The thermometer has been calibrated in the range from 273.15 to 873.15 K. The experimental uncertainties in the temperature measurements are within ± 0.01 K.

The pressures were measured with a dead-weight gauge, suitable for pressures from 1 to 100 MPa, combined with the stainless-steel diaphragm-type null indicator, which has a diameter of 30 mm and a thickness of 0.2 mm. The total uncertainty in the pressure measurements is less than ± 0.002 MPa.

For analysis small samples of 0.5 to 1 g in the homogeneous phase were bled into an evacuated and calibrated glass vessel. These samples were then cooled to $-78°C$ to determine the amount of water with a cathetometer. The total uncertainty in the concentration measurements does not exceed ± 0.002 mol fraction.

The hydrocarbons and nitrogen used had purities better than 99.85 %. These purities were checked by gas chromatography. The water was degassed and had a specific conductance of about $10^{-6}\,\Omega^{-1}\cdot cm^{-1}$. Both compounds were distilled and degassed at low pressure.

3. RESULTS

The experiments have been performed at five temperatures, namely, at 523.15, 573.15, 623.15, 653.15, and 663.15 K, in the homogeneous vapor phase. The experimental P–ρ–T–x data are presented in Tables I–V. Throughout this paper the concentration x refers to the mode fraction of water. As a check of the accuracy of our measurements, we also obtained P–ρ–T data for pure water, *n*-hexane, *n*-octane, and benzene at 523.15 K. A comparison of the new measurements with data previously reported for water in the literature [32] is shown in Table VI.

Each isotherm consists of 20 data points obtained at four compositions. The density ranges from 1 to 5 $kg \cdot m^{-3}$, with a maximum pressure of approximately 70 MPa. Some experimental results are shown in Figs. 1 and 2 as projections at constant composition (isopleths) in the P–ρ and Z–P planes, where $Z = PV/RT$ is the compressibility factor. A total of 65 data points at 17 concentrations for each system was obtained in this range.

Table I. Experimental Results for Nitrogen + Water

T (K)	P (MPa)	ρ ($kg \cdot m^{-3}$)	x (mole fraction water)
523.15	3.92	20.7	0.7316
	2.08	10.4	0.7316
	3.58	20.1	0.4340
	2.11	11.6	0.4340
	3.54	21.6	0.1477
	2.07	11.7	0.14477
	16.32	96.7	0.0585
	11.97	72.9	0.0585
	8.06	50.2	0.0585
	4.09	26.2	0.0585
573.15	8.16	40.3	0.8827
	5.56	25.3	0.8827
	2.58	11.0	0.8827
	8.17	40.0	0.778
	5.72	26.1	0.7781
	2.58	11.5	0.7781

Table I. *(Continued)*

T (K)	P (MPa)	ρ (kg · m^{-3})	x (mole fraction water)
	8.04	40.0	0.5239
	5.53	27.1	0.5239
	2.59	12.6	0.5239
	8.00	42.1	0.2540
	5.54	29.3	0.2540
	2.60	13.9	0.2540
	32.96	166.4	0.1179
	24.84	129.2	0.1179
	16.91	90.4	0.1179
	10.11	56.1	0.1179
	5.07	28.8	0.1179
663.15	59.83	506.0	0.9346
	50.81	456.5	0.9346
	40.99	368.4	0.9346
	31.53	230.7	0.9346
	20.68	101.8	0.9346
	10.45	40.9	0.9346
	5.62	20.3	0.9346
	60.04	362.1	0.8186
	49.68	299.5	0.8186
	39.86	227.9	0.8186
	29.83	151.7	0.8186
	19.79	87.6	0.8186
	10.00	39.2	0.8186
	5.05	18.8	0.8186
	60.80	274.6	0.6262
	49.43	224.9	0.6262
	39.55	178.6	0.6262
	29.64	130.7	0.6262
	19.76	84.3	0.6262
	9.82	40.6	0.6262
	5.06	20.3	0.6262
	69.28	273.1	0.4544
	54.21	221.4	0.4544
	39.40	164.8	0.4544
	29.57	124.6	0.4544
	19.74	83.1	0.4544
	9.39	40.9	0.4544
	5.05	20.3	0.4544

4. CORRELATIONS

The low-pressure data can within their experimental accuracy be represented by a truncated virial expansion,

$$Z = 1 + B(T)\rho + C(T)p^2 \tag{1}$$

or

$$(Z-1)/\rho = B(T) = C(T)\rho \tag{2}$$

Table II. Experimental Results for *n*-Octane + Water

T (K)	P (MPa)	ρ (kg · m^{-3})	x (mole fraction water)
623.15	15.26	411.0	0.1531
	12.94	388.4	0.1531
	11.01	363.4	0.1531
	8.98	325.0	0.1531
	7.08	265.5	0.1531
	6.01	216.6	0.1531
	5.05	166.1	0.1531
	4.06	118.5	0.1531
	3.08	79.6	0.1531
	14.92	372.9	0.2824
	11.96	329.4	0.2824
	9.06	260.5	0.2824
	6.02	154.0	0.2824
	4.55	104.6	0.2824
	3.06	62.9	0.2824
	14.83	307.5	0.4551
	12.88	269.9	0.4551
	10.95	225.5	0.4551
	8.97	176.0	0.4551
	6.02	105.4	0.4551
	4.54	74.5	0.4551
	3.08	47.6	0.4551
	14.95	169.8	0.7677
	11.94	122.8	0.7677
	9.01	85.2	0.7677
	6.02	52.8	0.7677
	4.60	39.0	0.7677
	3.08	25.4	0.7677

The values of the second virial coefficients $B(T)$ and the third virial coefficient $C(T)$ were determined by fitting our experimental compressibility factors Z to Eq. (2). If $(Z-1)/\rho$ is plotted as a function of ρ, Eq. (2) should yield a straight line with $B(T)$ as the intercept in the limit $\rho \to 0$ and with $C(T)$ as the slope. The values thus obtained for $B(T)$ at $T = 623.15$ K for the mixtures are shown in Fig. 3 as a function of the mole fraction x of H_2O.

The excess molar volume V^E is defined as

$$V^E(T, P, x) = V_m(T, P, x) - xV_1(T, P, 0) - (1-x)\, V_2(T, P, 1) \qquad (3)$$

Table III. Experimental Results for Benzene + Water

T (K)	P (MPa)	ρ (kg·m^{-3})	x (mole fraction water)
623.15	15.09	447.5	0.0688
	13.42	417.3	0.0688
	11.94	380.4	0.0688
	10.50	329.2	0.0688
	8.98	255.6	0.0688
	7.51	183.1	0.0688
	6.00	125.7	0.0688
	4.54	84.3	0.0688
	2.57	42.0	0.0688
	15.16	396.3	0.1685
	12.69	331.1	0.1685
	11.00	270.0	0.1685
	8.96	191.7	0.1685
	7.02	130.6	0.1685
	5.06	83.1	0.1685
	2.56	37.2	0.1685
	15.04	293.5	0.3607
	12.91	233.7	0.3607
	10.75	176.2	0.3607
	8.99	135.5	0.3607
	7.02	97.0	0.3607
	5.04	64.5	0.3607
	2.57	30.3	0.3607
	15.20	155.5	0.7241
	12.84	119.4	0.7241
	10.99	95.9	0.7241
	8.96	73.6	0.7241
	7.02	54.8	0.7241
	5.01	37.4	0.7241
	2.63	18.7	0.7241

Table IV. Experimental Results for Methane + Water

T (K)	P (MPa)	ρ (kg · m^{-3})	x (mole fraction water)
523.15	4.94	23.18	0.7900
	2.63	11.43	0.7900
	5.69	25.97	0.6777
	2.64	10.95	0.6777
	6.54	29.46	0.5358
	2.64	10.02	0.5358
573.15	8.10	35.47	0.8159
	4.69	19.04	0.8159
	2.24	8.64	0.8159
	8.33	33.37	0.6561
	4.69	18.00	0.6561
	2.25	8.35	0.6561
	8.43	31.14	0.4567
	4.71	17.08	0.4567
	2.26	8.02	0.4567
	30.12	119.07	0.4326
	25.11	94.87	0.4326
	19.79	73.71	0.4326
	15.20	55.70	0.4326
	10.01	35.88	0.4326
	5.16	18.14	0.4326
	8.39	28.97	0.2301
	4.89	16.14	0.2301
	2.24	7.74	0.2301
623.15	13.85	57.1	0.8116
	10.50	40.9	0.8116
	8.02	29.9	0.8116
	4.14	14.6	0.8116
	13.81	48.6	0.5593
	10.48	36.2	0.5593
	7.49	25.5	0.5593

Table IV. *(Continued)*

T (K)	P (MPa)	ρ (kg · m^{-3})	x (mole fraction water)
	14.11	46.3	0.3761
	10.93	35.7	0.3761
	7.50	24.4	0.3761
	4.04	13.2	0.3761
	15.13	46.6	0.1527
	11.08	34.1	0.1527
	7.96	24.8	0.1527
	4.07	12.6	0.1527
653.15	59.69	539.9	0.9555
	32.14	309.0	0.9555
	25.84	176.1	0.9555
	20.35	104.6	0.9555
	59.60	355.3	0.8424
	40.56	236.0	0.8424
	18.10	73.8	0.8424
	10.86	39.8	0.8424
	6.58	29.9	0.8424
	3.26	10.9	0.8424
	59.58	304.9	0.7900
	50.18	258.2	0.7900
	40.21	199.3	0.7900
	31.56	144.3	0.7900
	20.87	83.6	0.7900
	60.41	188.9	0.4914
	41.02	133.5	0.4914
	21.72	69.8	0.4914
	11.43	39.0	0.4914
	8.31	21.1	0.4914
	63.24	177.2	0.3709
	43.28	127.0	0.3709
	23.09	69.6	0.3709
	12.32	37.0	0.3709
	7.64	22.4	0.3709

Table V. Experimental Results for *n*-Hexane + Water

T (K)	P (MPa)	ρ (kg · m^{-3})	x (mole fraction water)
523.15	7.07	374.4	0.0602
	6.10	350.3	0.0602
	5.09	304.5	0.0602
	4.60	259.3	0.0602
	4.11	190.2	0.0602
	3.59	131.2	0.0602
	3.00	90.8	0.0602
	2.13	54.5	0.0602
	4.04	107.2	0.1928
	3.55	86.9	0.1928
	3.05	70.1	0.1928
	2.10	43.6	0.1928
	4.05	66.0	0.4396
	3.03	46.2	0.4396
	2.10	30.7	0.4396
	4.19	42.2	0.7231
	2.10	19.6	0.7231
573.15	7.96	265.1	0.0813
	7.04	227.9	0.0813
	6.04	181.8	0.0813
	5.04	136.3	0.0813
	4.05	97.9	0.0813
	2.10	42.4	0.0813
	7.97	226.1	0.1558
	6.96	187.7	0.1558
	6.04	152.1	0.1558
	4.06	86.1	0.1558
	2.12	39.0	0.1558

Table V. *(Continued)*

T (K)	P (MPa)	ρ (kg · m^{-3})	x (mole fraction water)
	8.07	137.9	0.4101
	6.05	94.3	0.4101
	4.08	58.5	0.4101
	2.12	28.5	0.4101
	8.25	83.7	0.6997
	6.05	56.6	0.6997
	4.01	35.3	0.6997
	2.16	18.2	0.6997
623.15	14.84	317.8	0.1074
	12.94	290.3	0.1074
	10.86	251.3	0.1074
	8.98	206.4	0.1074
	6.03	125.2	0.1074
	3.11	55.3	0.1074
	15.01	273.6	0.2620
	12.92	239.1	0.2620
	10.97	201.7	0.2620
	8.98	159.7	0.2620
	6.03	98.2	0.2620
	3.08	45.2	0.2620
	15.12	196.6	0.5174
	11.97	149.4	0.5174
	8.97	105.5	0.5174
	6.04	66.7	0.5174
	3.10	32.3	0.5174
	15.05	126.0	0.8031
	11.95	91.4	0.8031
	8.97	63.7	0.8031
	6.02	40.2	0.8031
	3.13	20.0	0.8031

where V_m is the measured volume of the mixture at temperature T, pressure P, and concentration x and where V_1 and V_2 are the molar volumes of the pure components at the same temperature T and pressure P. Figure 4 shows the molar volume V_m for water + methane and the corresponding partial molar volumes $\bar{V}_1$ and $\bar{V}_2$ and excess volume V^E as a function of x at constant temperature for water + methane and water + nitrogen. Figure 5 shows V^E at constant temperature and at various pressures for water + methane and water + nitrogen. The behavior of V^E as a function of pressure at constant composition is shown in Fig. 6 for water + nitrogen. A comparison of our experimental results for water + methane with previous results reported by Christoforakos and Franck [28, 33] is shown in Fig. 7.

The values of V^E in the zero-pressure limit are represented by

$$V^E(T, P \to 0, x) = x(1-x)[2B_{12}(T) - B_{11}(T) - B_{22}(T)] \tag{4}$$

where B_{11} and B_{22} are the second virial coefficients of the pure components and B_{12} is a cross second virial coefficient. The behavior of B_{12} of water + methane as a function of temperature is shown in Fig. 8.

From the values of V^E as a function of pressure, the excess Gibbs free energy G^E can be determined as

$$G^E(T, P, x) = \int_0^P V^E(T, P', x)\, dP' \tag{5}$$

The results thus obtained for G^E of the mixtures at $T = 663.15$ K as a function of the water more fraction x are shown in Fig. 9. The Redlich–Kister equation has been used to represent the excess Gibbs free energies as

$$G^E = x_1 x_2 [A + B(x_1 - x_2)] \tag{6}$$

Table VI. Comparison of the New Experimental P–ρ–T Data with Previous Results for Pure Water at 623.15 K

P (MPa)	ρ^a (kg·m^{-3})	ρ^b (kg·m^{-3})	Deviation (%)
14.61	82.00	82.19	−0.23
11.31	52.26	53.10	−0.26
7.98	33.33	33.24	+0.27
6.81	27.38	27.44	−0.22
4.21	15.78	15.93	−0.95

[a] From this work.
[b] From Ref. 32.

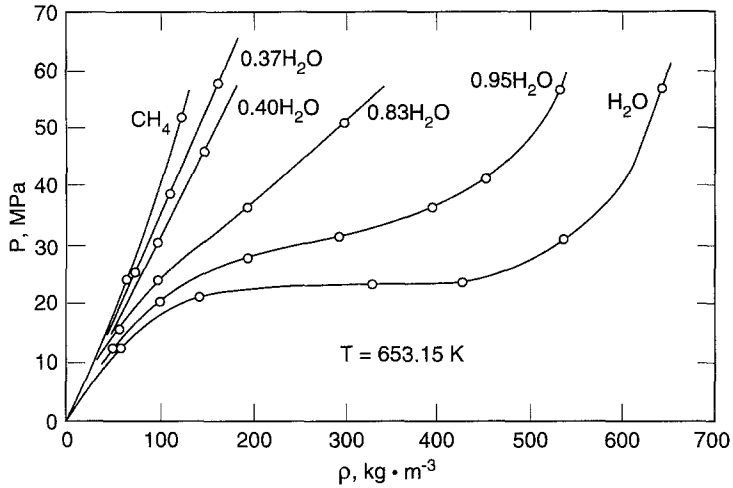

Fig. 1. P–ρ curves at constant composition (isopleths) for water + methane in the homogeneous supercritical region at $T = 653.15$ K.

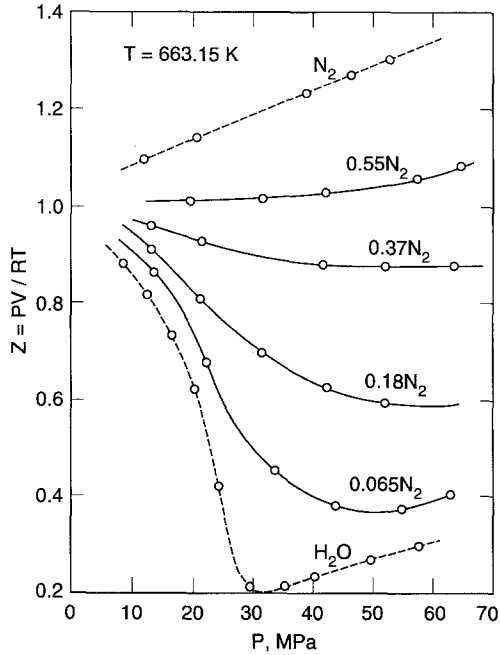

Fig. 2. Compressibility factor $Z = PV/RT$ as a function of pressure P for water + nitrogen at various concentrations in the homogeneouos supercritical region at $T = 663.15$ K.

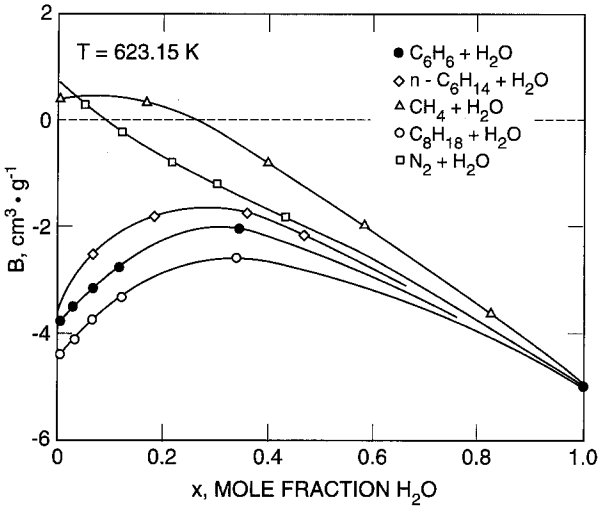

Fig. 3. The second virial coefficient $B(T)$ at $T = 623.15$ K for water + nitrogen and water + hydrocarbon mixtures.

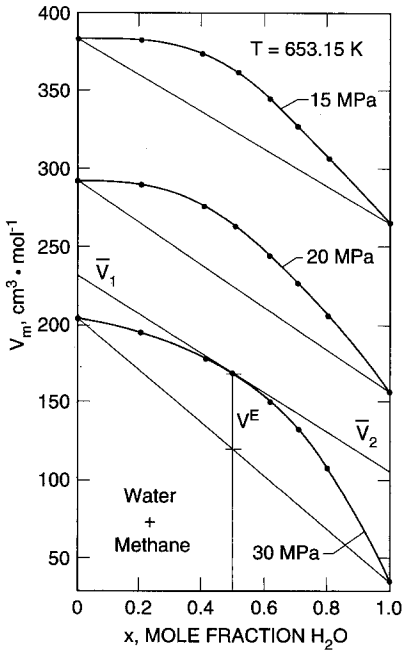

Fig. 4. Molar volume V_m as a function of concentration x for water + methane in the homogeneous supercritical region at $T = 653.15$ K at a number of pressures. $\bar{V}_1$ and $\bar{V}_2$ are the partial molar volumes and V^E is the excess volume.

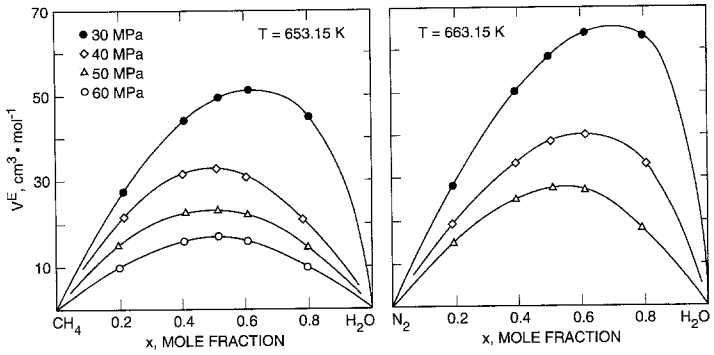

Fig. 5. Excess molar volume V^E as a function of concentration x at constant temperature for water + methane and water + nitrogen.

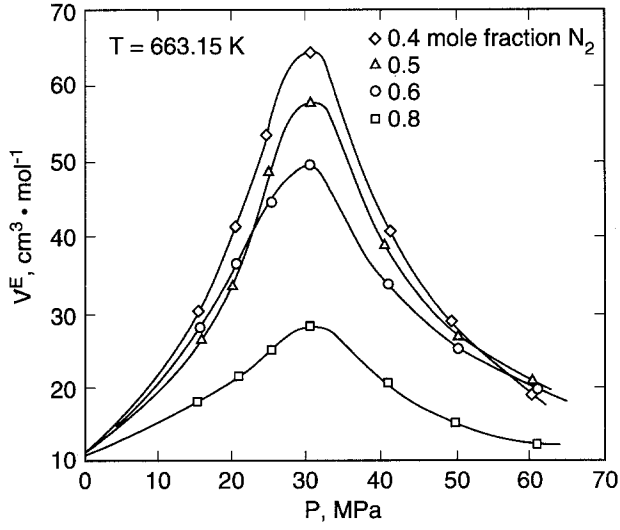

Fig. 6. Excess molar volume V^E at $T = 663.15$ K as a function of pressure for water + nitrogen at various values of x.

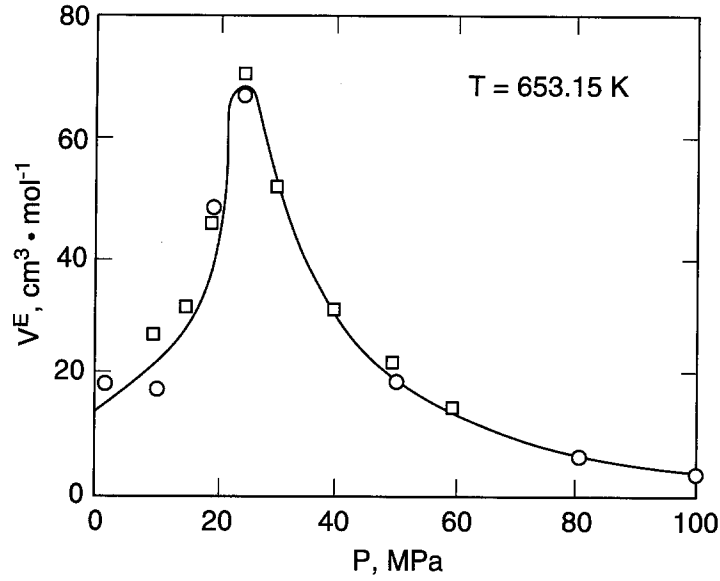

Fig. 7. Excess molar volume V^E at $T = 653.15$ K as a function of pressure for water + methane at $x = 0.6$ mol fraction H_2O. The squares indicate our experimental data. The circles and the solid curve represent experimental and calculated values reported by Christoforakos and Franck [28, 33].

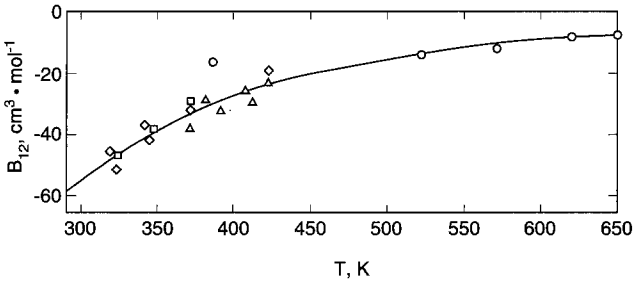

Fig. 8. Cross second virial coefficient for water + methane as a function of temperature. (○) This work; (□) Ref. 34, (△) Ref. 35; (◇) Ref. 36. The solid curve represent values calculated from the equation of state of Christoforakos and Franck [33].

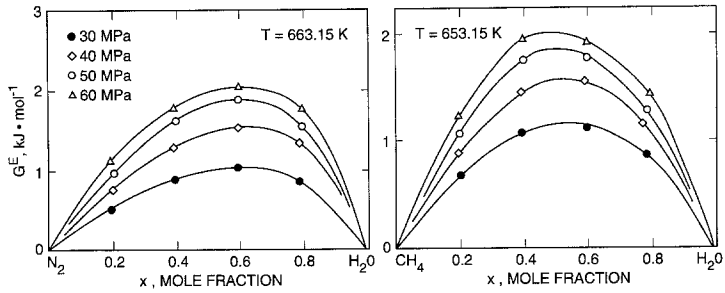

Fig. 9. Excess Gibbs free energy G^E as a function of x at constant temperature for water + nitrogen and water + methane for various pressures.

Table VII. Values for the Constants A and B in the Excess Gibbs Energy Equation, Eq. (7), for Water + Nitrogen and Water + Methane at 663.15 K

P (MPa)	A (kJ · mol^{-1})	B (kJ · mol^{-1})
	Water + nitrogen	
10	0.51216	0.06339
20	1.62728	0.37625
30	3.65249	1.47837
40	5.66787	2.64889
50	6.86711	2.94131
60	7.77904	2.99611
	Water + methane	
5	0.49249	−0.05191
10	1.01418	−0.14635
15	1.57746	−0.19709
20	2.27208	−0.20138
25	3.35449	0.31710
30	4.55572	1.00009
40	6.17691	1.09986
50	7.27033	0.97442
60	7.98133	0.90891

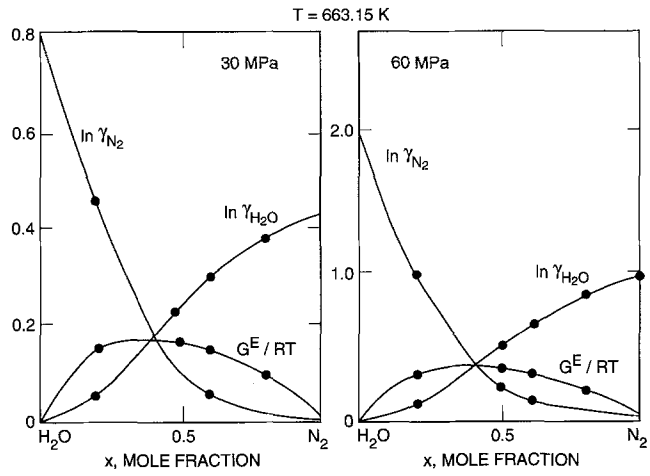

Fig. 10. Activity coefficients and G^E/RT at $T = 663.15$ K as a function of x for water + nitrogen at $P = 30$ and 60 MPa.

where x_1 and $x_2 = 1 - x$ are the mole fraction of the two components in the mixture. The values obtained for the coefficients A and B at $T = 663.15$ K for water + nitrogen and water + methane as a function of pressure are presented in Table VII. The activity coefficients γ_1 and γ_2 of the two components in the mixture can be calculated from

$$RT \ln \gamma_1 = x^2[A + B(3 - 4x)] \tag{7}$$

$$RT \ln \gamma_2 = (1 - x)^2[A + B(1 - 4x)] \tag{8}$$

where $x = x_2$. The results obtained for G^E/RT and the activity coefficients of water + nitrogen at 30 and 60 MPa are shown in Fig. 10.

5. CONCLUSION

We have obtained new P–ρ–T–x data for five binary aqueous systems at supercritical conditions, namely, for water + nitrogen and for several water + hydrocarbon mixtures. These experimental results can be used to develop and test theoretical models for the equation of state of binary mixtures near the critical point. A truncated virial expansion can be used

to represent the compressibility factor of water + hydrocarbon mixtures at densities from 0 to $0.5\rho_c(x)$.

From the experimental P–ρ–T–x data we have deduced the excess Gibbs free energy and the activity coefficients for water + methane and water + nitrogen. These results can be used to test the asymptotic behavior of the activity coefficient near the solvent's critical point. It should be noted that Eq. (7) cannot be used near the critical point of the solvent and one needs to consider nonclassical equations for this purpose [37].

REFERENCES

1. J. M. H. Levelt Sengers, in *Supercritical Fluid Technology*, T. J. Bruno and J. F. Ely, eds. (CRC Press, Boca Raton, FL, 1992), p. 1.
2. G. M. Schneider, *Theory and Practice in Supercritical luid Technology* (NTS, Tokyo, 1987).
3. E. U. Franck and G. M. Schneider, *Ber. Bunsenges. Phys. Chem.* **88**:783 (1984).
4. R. W. Shaw, T. B. Brill, A. A. Clifford, C. A. Eckert, and E. U. Franck, *Chem. Eng. News* Dec. 23 (1991), p. 26.
5. G. C. Ulmer and H. L. Barnes, *Hydrothermal Experimental Techniques* (Wiley, New York, 1987).
6. J. M. H. Levelt Sengers, *Int. J. Thermophys.* **11**:399 (1990).
7. Th. W. de Loos, W. G. Penders, and R. N. Lichtenthaler, *J. Chem. Thermodynam.* **14**:83 (1982).
8. Th. W. de Loos, J. H. van Dorp, and R. N. Lichtenthaler, *luid Phase Equil.* **10**:279 (1983).
9. E. Brunner, *J. Chem. Thermodynam.* **22**:335 (1990).
10. S. B. Kiselev, I. G. Kostyukova, and A. A. Povodyrev, *Int. J. Thermophys.* **12**:877 (1991).
11. G. X. Jin, S. Tang, and J. V. Sengers, *Fluid Phase Equil.* **75**:1 (1992); *Phys. Rev. E* (in press).
12. M. A. Anisimov and S. B. Kiselev, *Int. J. Thermophys.* **13**:873 (1992).
13. K. Bröllos, K. Peter, G. M. Schneider, *Ber. Bunsenges. Physik. Chem.* **74**:682 (1970).
14. T. Yiling, Th. Michelberger and E. U. Franck, *J. Chem. Thermodynam.* **23**:105 (1991).
15. M. L. Japas and E. U. Franck, *Ber. Bunsenges. Phys. Chem.* **89**:783 (1985).
16. C. J. Rebert and W. B. Kay, *AIChE. J.* **5**:285 (1959).
17. H. Welsch, Ph.D. thesis (University of Karlsruhe, 1973).
18. R. G. Sultanov, B. G. Skripka, and A. Y. Namiot, *Gasov. Prom.* **17**:6 (1972).
19. A. Danneil, K. Tödheide, and E. U. Franck, *Chem.-Ing.-Tech.* **39**:816 (1967).
20. M. Sanchez and R. Coll, *Anal. Quim.* **74**:1329 (1978).
21. Th. W. de Loos, A. J. Wijen, and G. A. M. Diepen, *J. Chem. Thermodynam.* **12**:193 (1980).
22. J. F. Connolly, *J. Chem. Eng. Data* **11**:13 (1966).
23. K. H. Peter, Diplom thesis (University of Karlsruhe, 1968).
24. Z. Alwani and G. M. Schneider, *Ber. Nunsenges. Phys. Chem.* **71**:633 (1967).
25. C. J. Rebert and K. E. Hayworth, *AIChE J.* **13**:118 (1967).
26. D. S. Tsiklis and V. Y. Maslennikova, *Dokl. Akad. Nauk SSSR* **161**:645 (1965).
27. V. M. Prokhorov and D. S. Tsiklis, *Zh. Fiz. Khim.* **44**:1173 (1970).
28. M. Christoforakos, Ph.D. thesis (University of Karlsruhe, 1985).
29. D. S. Tsiklis and V. Y. Maslennikova, *Dokl. Akad. Nauk SSSR* **157**:426 (1964).
30. I. M. Abdulagatov, A. R. Bazaev, and A. E. Ramazanova, *Ber. Bunsenges. Phys. Chem.*, in press (1992).

31. A. R. Bazaev, V. G. Scripka, and Y. A. Namiot, *Neftepromislovoe delo* **10**:35 (1974).
32. V. V. Sytchev, A. A. Aleksandrov, and Z. A. Ershova, *Svoistva materialov i veshestv. Voda i vodaynoi par. (VNIC MV, Moskow)* **1**:49 (1990).
33. M. Christoforakos and E. U. Franck, *Ber. Bunsenges. Phys. Chem.* **90**:780 (1986).
34. M. Rigby and J. M. Prausnitz, *J. Phys. Chem.* **72**:330 (1968).
35. G. Smith, A. Sellars, T. K. Yerlett, and C. J. Wormald, *J. Chem. Thermodynam.* **15**:29 (1983).
36. Y. A. Namiot, *Rastvorimost gazov v vodo.* (Nedra, Moscow, 1991), p. 135.
37. R. F. Chang and J. M. H. Levelt Sengers, *J. Phys. Chem.* **90**:5921 (1986).